High Resolution Physical Characterization of Single Metallic Nanoparticles

AUTHORS & AFFILIATIONS:
Jessica Ettedgui[1,2], Jacob Forstater[1,2], Joseph W. Robertson [1], John J. Kasianowicz[1,3].

[1] Physical Measurement Laboratory
National Institute of Standards and Technology
100 Bureau Drive, Gaithersburg, MD 20899

[2] Department of Chemical Engineering
Columbia University
550 West 120th Street, New York, NY 10027-6623

[3] Department of Applied Physics and Applied Math
Columbia University
550 West 120th Street, New York, NY 10027-6623

E-MAIL ADDRESSES:
Jessica Ettedgui   jessica.benjamini@nist.gov, jb3879@columbia.edu
Jacob Forstater   jacob.forstater@nist.gov
Joseph W. Robertson joseph.robertson@nist.gov
John J. Kasianowicz   john.kasianowicz@nist.gov

CORRESPONDING AUTHOR: Jessica Ettedgui

KEYWORDS:
Nanopore, α-Hemolysin, Lipid bilayer, Single-molecule analysis, Polyoxometalates, Isomers.

SHORT ABSTRACT:
Discrete metal oxygen clusters, polyoxometalates (POMs), can be detected at the single molecule limit using a biological nanopore-based electronic platform. The method provides a complementary approach to traditional analytical chemistry tools utilized in the study of these molecules.

LONG ABSTRACT:
It was shown earlier that individual molecules can be detected and characterized by measuring the degree by which they reduce the ionic current flowing through a single nanometer-scale pore. The signal is characteristic of the molecule's physicochemical properties and its interactions with the pore.

We demonstrate that the nanopore formed by the bacterial protein exotoxin *Staphylococcus aureus* alpha hemolysin can detect polyoxometalates (POMs), anionic metal oxygen clusters, at the single molecule limit. Moreover, multiple degradation products of 12-phosphotungstic acid POM (PTA, $H_3PW_{12}O_{40}$) in solution are simultaneously measured. The single molecule sensitivity of the nanopore method allows POMs to be characterized at significantly lower concentrations than those required for NMR spectroscopy.

This technique could serve as a new tool for chemists to study the molecular properties of polyoxometalates or other metallic clusters, to better understand POM synthetic processes, and possibly improve their yield. Conceivably, the location of a given atom, or the rotation of a fragment in the molecule, and the metal oxidation state could be investigated with this method. In addition, this new technique has the advantage of allowing the real-time monitoring of molecules in solution. The single molecule sensitivity of the nanopore method allows for POMs to be characterized at significantly lower concentrations than required for NMR spectroscopy and other techniques.

INTRODUCTION:

Detecting biomolecular analytes at the single molecule level can be performed by using nanopores and measuring ionic current modulations. Typically, nanopores are divided into two categories based on their fabrication: biological (self-assembled from protein or DNA origami) [1,2], or solid-state (e.g., manufactured with semiconductor processing tools) [3,4]. While solid-state nanopores were suggested as potentially more physically robust and offer a wide range of permissible solution conditions, protein nanopores thus far offer greater sensitivity, more resistance to fouling, greater bandwidth, better chemical selectivity, and a greater signal to noise ratio.

A variety of protein ion channels, such as the one formed by *Staphylococcus aureus* α-hemolysin (αHL), can be used to detect single molecules, including ions (e.g., H^+ and D^+)[1,2], polynucleotides (DNA and RNA) [5-7], damaged DNA[8], polypeptides[9], proteins (folded and unfolded) [10], polymers (polyethylene glycol and others) [11-13], gold nanoparticles[14-18] and other synthetic molecules.[19].

We recently demonstrated that the αHL nanopore can also easily detect and characterize metallic clusters, polyoxometalates (POMs) at the single molecule level. POMs are discrete nanoscale anionic metal oxygen clusters that were discovered in 1826[20], and since then, many other types have been synthesized. The different sizes, structures, and elemental compositions of polyoxometalates led to a wide range of properties and applications including chemistry[21,22], catalysis,[23] material science, [24 25] and biomedical research. [26,27 28]

POM synthesis is a self-assembly process typically carried out in water by mixing the stoichiometric amounts of monomeric metal salts. Once formed, POMs exhibit a great diversity of well-defined sizes and shapes. For example, the Keggin polyanion structure, $XM_{12}O_{40}{}^{q-}$ is

composed of one heteroatom (X) surrounded by four oxygens to form a tetrahedron (where q is the valence). The heteroatom is centrally located within a cage formed by 12 octahedral MO_6 units (where M = transition metals in their high oxidation state), which are linked to one another by neighboring shared oxygen atoms. While the structure of tungsten polyoxometalates is stable in acidic conditions, hydroxide ions lead to the hydrolytic cleavage of metal-oxygen (M-O) bonds.[29] This complex process results in the loss of one or more MO_6 octahedral subunits, leading to the formation of monovacant and trivacant species and eventually to the POM complete decomposition. Our discussion will be limited to the partial decomposition products of 12-phosphotungstic acid at pH 5.5 and 7.5.

While tungsten polyoxometalates structure is stable in acidic conditions, hydroxide ions lead to its decomposition.[29] This complex process is triggered by hydrolytic cleavage of the metal-oxygen (M-O) bonds and therefore the loss of one or three MO_6 octahedral subunits, leading to the formation of monovacant and trivacant species. Our discussion will be limited to the partial decomposition products of 12-phosphotungstic acid at pH 5.5 and 7.5.

The nanopore-based analytical method allows simultaneous determination of multiple species in solution with greater sensitivity than conventional methods. With it, subtle differences in POM structure can be elucidated, and at concentrations markedly lower than those required for NMR spectroscopy. Importantly, this approach even allows the discrimination of isomeric forms of $Na_8HPW_9O_{34}$.[30]

PROTOCOL:
The protocol below is specific to the Nanopatch^{TM} DC System (Electronic Biosciences, Inc., EBS). However, it can be readily adapted to other electrophysiology instrumentation used to measure the current through planar lipid bilayer membranes (standard lipid bilayer membrane chamber, U-tube geometry, pulled microcapillaries, Ionera MEKA chips for a Nanion Orbit 16, etc.). The identification of commercial materials and their sources is given to describe the experimental results. In no case does this identification imply recommendation by the National Institute of Standards and Technology, nor does it imply that the materials are the best available.

1. Solution and Analyte Preparation
1.1 Buffered Electrolyte
All electrolyte solutions are prepared with 18 MΩ-cm water from a Type-1 water purification system with Millipore LC-PAK final filter to remove trace organics species and then filtered through a 0.22 μm Millipore vacuum filter immediately before ion channel recordings. The water quality is a <u>critical</u> factor for the stability and longevity of the membrane nanopore system.

1.2 Wild Type αHL
1. Follow MSDS precautions when handling the αHL toxin.
2. Mix lyophilized wild-type monomeric *S. aureus* α-Hemolysin (αHL, List labs, Inc.) powder with 18 MΩ-cm water at 1 mg/mL and stored in 10 to 30 μL aliquots in sterilized 1.5 mL Eppendorf tubes at -80°C. Alternatively, purified preformed heptameric *α*HL could be used. [31]

1.3 Lipids.
Dissolve the lipid 1,2-Diphytanoyl-sn-Glycero-3-Phosphocholine (DPhyPC, Avanti Polar Lipids, Alabaster, AL) to 0.2 mg/mL in *n*-decane (Sigma-Aldrich) and stored in a 4 mL glass scintillation vial with a Teflon-coated cap. The solution is stored at ~ 4°C for up to one month during repeated use.

1.4 Phosphotungstic acid solutions.
Prepare 2 mM phosphotungstic acid stock solution by dissolving 57.6 mg of $H_3PW_{12}O_{40}$ into 10 mL of a 1 M NaCl and 10 mM NaH_2PO_4 solution, and adjust the pH to 5.5 with 3 M NaOH. At this pH value, 12-phosphotungstic acid (PTA, $H_3PW_{12}O_{40}$) decomposes primarily into the monovacant anion $[PW_{11}O_{39}]^{7-}$.

2. Test Cell Assembly
1. The test cell should be assembled per the EBS manufacturer's instructions.
2. Soak one Ag/ AgCl wire in bleach (sodium hypochlorite) for 10 minutes after abrading it with sandpaper (600 grit). Position the electrode inside the quartz nanopore membrane (QNM).
3. Place a cylindrical AgCl pellet electrode embedded in a silver wire outside of the quartz nanopore membrane (QNM).
4. Once the test cell is set up, the power supply and data acquisition program should be turned on. The DC current reading should be 0 pA in the absence of solution in the test cell.
5. Use a syringe connected to the test cell via a fluid line to add buffered electrolyte solution above the face of the QNM and to ensure that the ionic current saturates the amplifier. If it does not, the QNM may be clogged. Apply a "pop voltage" (+/- 1 V) and/or a pressure greater than 300 mm Hg to try and clear it. If this works, remove the voltage and pressure.

3. Lipid Bilayer Formation
1. Fill the solution in the test cell so that the solution level is well above the face of the QNM and can then be lowered via syringe to below the face, such that the current decreases to zero.
2. Dip a 10 μL pipette tip into the lipid vial. Push on the back end of the pipette tip and tap it on the side of the vial to remove all visible lipid. Touch the pipette tip onto the air-water interface of the solution in the test cell when the solution level is above the QNM's face and wait two to five minutes for a lipid monolayer to spread uniformly. Slowly lower the solution level below the face of the QNM until the current saturates, and then slowly raise the solution level past the face of the QNM to form a lipid bilayer. Once a bilayer appears to form (i.e., when the current goes to zero), try popping it several times by increasing the pressure and ensure the QNM is not merely clogged.
3. If the bilayer did not form the first time, lower the solution below the QNM and raise it again.
4. After forming a membrane, set the current offset to zero when the applied potential is zero.

4. *α*-HL Pore Formation
1. Add 2.5 ng of purified preformed *α*HL heptameric protein sample to the test cell (volume ≈

200 μL) to enable insertion of the protein or alternatively ≈ 250 ng of monomeric αHL (List Biological Laboratories, Campbell, CA)

2. Increase the pressure on the bilayer with a gas-tight syringe (Fig. 1) after a bilayer is formed, to expand the membrane from the QNM, which aids nanopore formation. The applied back pressure is typically raised between 40 to 200 mmHg, depending on each QNM. The EBS software has an automated insertion feature that applies a higher bias (typically 200 to 400 mV) to induce pore formation and then automatically reduces the desired voltage to the measurement bias once a pore forms.

3. After a single channel forms, reduce the back pressure to about 1⁄2 of the insertion pressure. If multiple channels are observed, significantly reducing the back pressure will usually remove them.

5. Metallic Cluster Partitioning in the Nanopore

1. Set the dc offset to ensure that there is no ionic current flowing when no voltage is applied (to eliminate electrode imbalances).

2. Prior to adding the POM sample, perform a control experiment to ensure there are no contaminants (e.g., trace POMs from a previous experiment) in the reservoir. Specifically, acquire a current trace under an applied potential of +120 mV to -120 mV in the absence of any to verify that no spurious current blockades are detected. The degree by which α-HL preferentially conducts in one direction is called the rectification ratio, which can be used to determine the orientation of the αHL nanopore insertion.

3. Add the POM sample by flushing the reservoir with metallic cluster solution at 1 to 5 μM concentration. The sample can instead be loaded into the capillary prior to cell assembly.

4. Record the ionic current using software to detect transient current blockades as individual molecules partition into the nanopore. The blockade depth, duration, and frequency of the blockades (analyzed off line) provide information about the POM's physical and chemical properties.

6. Ion Channel Recordings and Data Analysis

A custom-built, high-impedance, low-noise amplifier and data acquisition system, designed and constructed by EBS, was used to record the ionic current time series. The measurements are performed at -120mV (relative to channel *cis* side) for each pH. The data are recorded with a 100 kHz 8-pole Bessel filter and digitized at 500 kHz (i.e., 2 μs/point). Events are extracted from the ionic current time series and analyzed using the ADEPT algorithm in the *MOSAIC* software package.[32]

REPRESENTATIVE RESULTS:

Figure 1: Schematic diagram of the experimental setup

For over the past two decades, membrane-bound protein nanometer-scale pores have been demonstrated as versatile single-molecule sensors. Such nanopore measurements are conceptually simple: two chambers filled with electrolyte solution are separated by a nanopore embedded in an electrically insulating lipid membrane. Either a patch-clamp amplifier or an

external power supply applies an electrostatic potential gradient across the nanopore via Ag/AgCl electrodes immersed in the electrolyte reservoirs. The electric field drives individual charged particles into the pore, which produces transient reductions in the ionic current that depend on the particle size and shape, as well as the charge that reversibly binds to the molecule. A computer program controls the applied voltage and monitors, in real time, the ionic current blockades caused by molecules that reversibly partition into the pore. The current is amplified and converted to voltage with a high impedance field-effect transistor.

Figure 2: Nanopore-based detection of individual metallo-nanoparticles
Here, we provide a general procedure for detecting polyoxometalates with a biological nanopore. The ionic current time series (Fig. 2) shows the open channel current ($\approx$ 100 pA) under an applied potential of -120 mV in the absence and presence of POMs. Individual POMs decrease the ionic current by $\approx$ 80 % and the current blockades are not observed when the applied potential polarity is reversed, which is consistent with the POMs' negative charge. Note that if the POMs didn't interact with the pore wall, they would electrodiffuse the pore's length in $\approx$ 100 ns, which is too brief to be detected with a conventional patch clamp amplifier. Thus, most of the time a given molecule spends in the pore is a direct consequence of the interaction between it and the pore. The duration of an ionic current blockade event, τ, is defined as the residence time of the molecule in the pore.

Figure 3: Histograms of the current blockade depth ratio at pH 5.5 and 7.5
To illustrate the utility of this method, we discuss the use of the αHL nanopore to monitor the partial decomposition of 12-phosphotungstic acid (PTA, $H_3PW_{12}O_{40}$) at pH 5.5 and pH 7.5. At these pH values, stock solutions ([PTA] = 2 mM) were first measured with ^{31}P NMR prior to further dilution to 30 μM for the nanopore-based measurements. At pH 5.5, $[PW_{11}O_{39}]^{7-}$ is the predominant species.[29]

The data analysis is performed by calculating a histogram of the blockade depth ratio (i.e., $\langle i \rangle / \langle i_o \rangle$, where $\langle i \rangle$ is the mean current with the POM in the pore and $\langle i_o \rangle$ is the mean open channel current). The histogram of the mean current blockade depth ratios at -120 mV and pH 5.5 exhibits a minor peak at $\langle i \rangle / \langle i_o \rangle \approx 0.06$ and major peak at $\langle i \rangle / \langle i_o \rangle \approx 0.16$ (Fig. 3, *green*). We assume these peaks correspond to $[P_2W_5O_{23}]^{6-}$ and $[PW_{11}O_{39}]^{7-}$, respectively.

When the POM solution is titrated to pH 7.5, the total POM concentration decreases due to the partial degradation of the two principal species (as expected from the results of conventional analysis) to inorganic salts (i.e., free phosphate, $H_xPO_4^{-3+x}$ and tungstate, WO_4^{2-} ions). The histogram of the blockade depth ratio also shows two principal peaks (Fig. 3, *orange*), but with 20-fold fewer events per unit time (which suggests the total POM concentration at pH 7.5 is $\approx$ 20-fold less than that at pH 5.5, if the nanopore's capture efficiency for POMs is the same at the two pH values). It is interesting to note that at pH 7.5 and greater, the POM species observed here were not detected in the ^{31}P NMR spectrum due to their low concentration caused by their dissociation into phosphate and tungstate ions.

Figure 4: Residence time data fitting with several exponentials.
Each event's residence time in the pore is defined by the duration of the individual ionic current blockades. The distribution of residence times provides insight into the different species that are present. It was shown earlier that for blockades caused by a differently-sized polymers of poly(ethylene glycol), the residence time distribution for each size of that polymer is well described by a single exponential. That result suggests the interaction of that polymer is a simple reversible chemical reaction.[11] [12,19]

Figure 4 illustrates the residence time distributions for the two peaks were well differentiated at pH 5.5 and 7.5. Two features are clear. First, under all conditions, multiple exponentials are required to fit each of the distributions, which suggests there are variations of the POMs within each species. Second, the residence times of the POMs in the pore are much shorter at pH 7.5 compared to those at pH 5.5, which imply a weakening interaction between the pore and POMs, but which provides an additional means to discriminate between the different species. It has been shown previously that following a change in pH will change the relative number of fixed charges in or near the αHL channel's lumen as well as cause possible structural changes in the pore caused by protons binding to amino acid side chains. These changes will directly alter the interactions with partitioning POMs inside the pore and therefore modify their residence time.[33]

Figure Legends:
Figure 1: Schematic diagram of the experimental setup
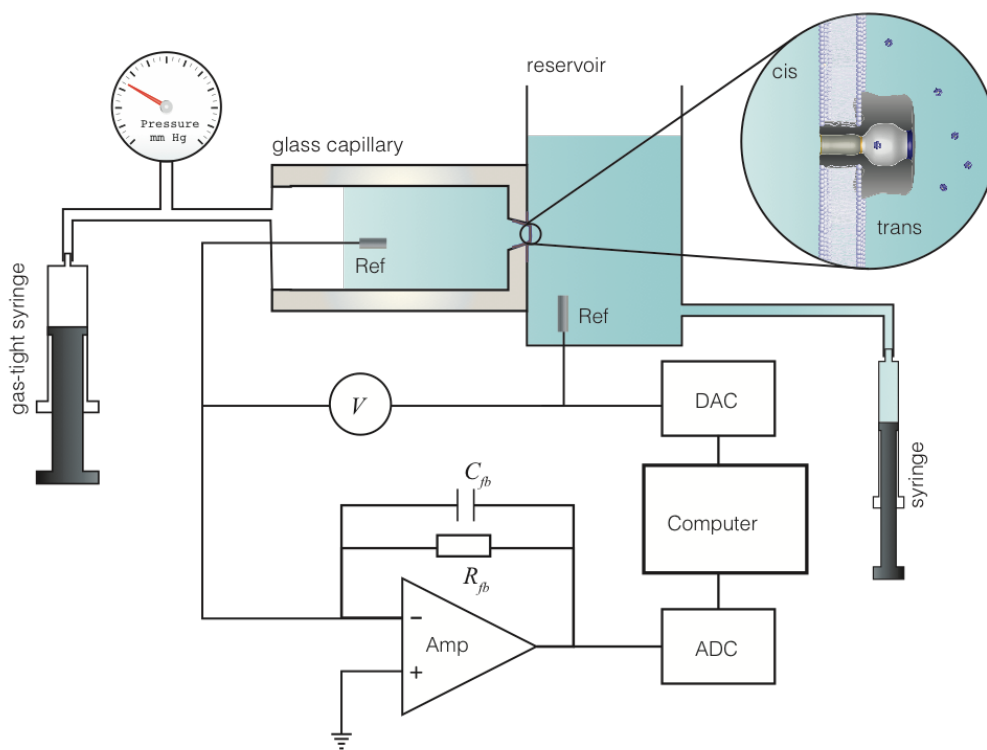
Method for nanopore-based characterization of individual polyoxometalate molecules. A protein

nanopore that self-assembles in a 4 nm thick lipid bilayer membrane is bathed by aqueous electrolyte solutions in a glass capillary and larger reservoir. A pressure is applied to the glass capillary with a gas-tight syringe to aid nanopore incorporation. An electrostatic potential V is applied across the membrane with a matched pair of Ag/AgCl electrodes and drives an ionic current (e.g., Na^+ and Cl^-) through the nanopore. The current is converted to voltage with a high impedance amplifier, digitized with an analog to digital converter (ADC) and stored on a computer. Computer software controls the applied potential through a digital to analog converter (DAC) and monitors, in real time, the transient current blockades caused by single molecules that partition into the pore.

Figure 2: Nanopore-based detection of individual metallo-nanoparticles


An illustration of ionic current time series traces that occur before and after the addition of a POM solution to the nanopore apparatus. The partitioning of individual anionic POMs into the pore causes transient current reductions in the mean open pore current, $<i_o>$. (*Right*) A typical event, illustrating the mean blockade depth ($<i>$) and the residence time (τ) of the particle in the pore. The applied potential was -120mV, and the solutions contained 1M NaCl, 10mM NaH_2PO_4 at pH 5.5. The *cis* compartment also contained 30 µM of 12-phosphotungstic acid. The current blockade depth ratio ($<i>/<i_o>$), and the residence times (τ) provide information about which POM species are present in solution.

Figure 3: Histograms of the current blockade depth ratio at pH 5.5 and 7.5.
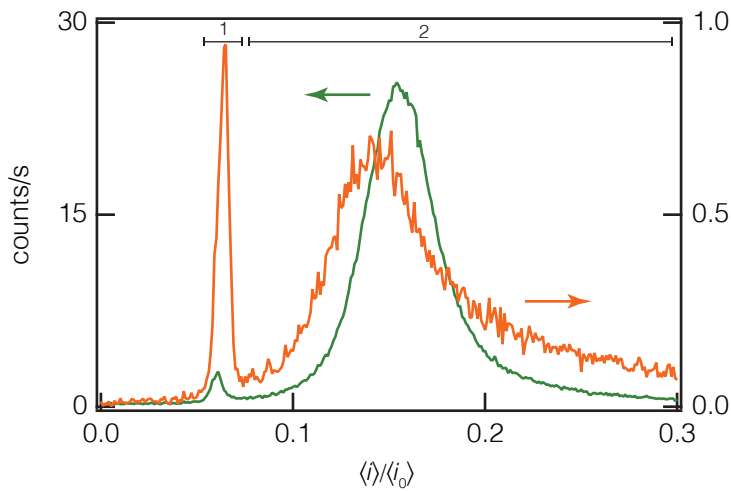
Histograms of the POM-induced ionic current blockade depth ratio at pH 5.5 (*green*) and 7.5 (*orange*) with an applied potential V = -120 mV. The two peaks present at each pH value correspond to the known predominate POM species in solution under those conditions. ^{31}P NMR studies suggest that increasing the pH changes the relative concentration of these two species, and this is borne out by the change in height of the two peaks shown above. The current blockade depth ratios of 0 and 1 correspond to a fully blocked and open pore, respectively. The histograms were created with a bin width of 0.001 (i.e., 1000 bins between 0 and 1) and normalized to counts/s by dividing by the data acquisition time.

Figure 4: Residence time distribution and fitting with several exponentials.
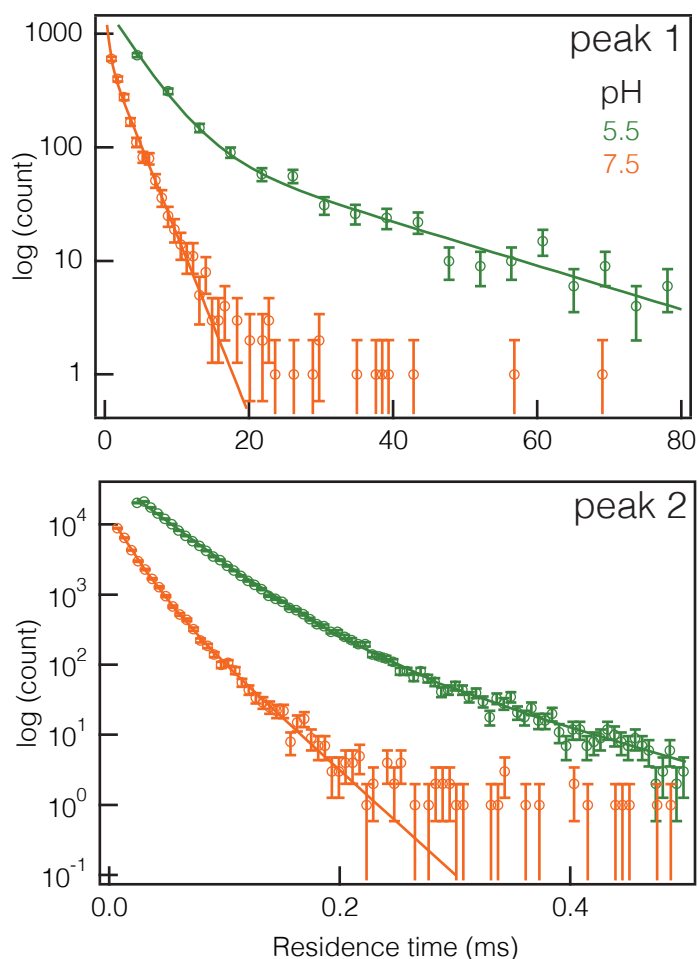
The distribution of residence times for POM-induced current blockades caused by the two principal species (peaks 1 and 2 in Fig. 3) observed at pH 5.5 and 7.5 in a semi-log plot. For both species, the residence times are markedly faster at the higher pH value, which suggests the interaction between the pore and POMs has changed. The solid lines are fits of an exponential mixture model to the data.

DISCUSSION:

Due to their anionic charge, POMs likely associate with organic counter cations through electrostatic interactions. Therefore, it is important to identify the proper solution conditions and the appropriate electrolyte solutions (especially cations) to avoid complex formation with POMs. For example, NaCl was purposely used instead of KCl (as well as the other alkali metals) to avoid the precipitation of $[PW_{11}O_{39}]^{7-}$ by K^+ containing electrolytes. Particular care is also required in the buffer choice. For example, the capture rate of POMs with TRIS and citric acid-buffered solutions is significantly lower than that in phosphate buffered solution, likely because the first two buffers form a complex with the POM, which doesn't interact with the nanopore.

Critical to the accurate measurement of the residence time distributions is the ability to measure the current at a sufficiently high bandwidth. For instance, with exponentially-distributed residence times there are far more blockades with relatively short than long residence times, and an accurate estimation of the residence time distributions is better achieved by collecting a great deal of data and acquiring it at as high a bandwidth the system's electrical capacitance allows. To achieve this condition in nanopore spectroscopy, the system capacitance (membrane and stray capacitance) should be minimized. Stray capacitance is reduced by decreasing the length of all connecting cables and using high quality electrical contacts and membrane capacitance is minimized by decreasing the surface area of the bilayer membrane, increasing the thickness of supporting materials (i.e., quartz, Teflon, etc.), and decreasing the area of exposed supporting materials to the electrolyte. In practice, a typical instrument's stray capacitance ($\approx$ 2 pF) will limit the noise for membranes $\approx$ 1 μm in diameter.

The structures and charges of polyoxometalates are currently studied using traditional analytical chemistry techniques, including nuclear magnetic resonance (NMR), mass spectrometry, X-ray diffraction, and spectroscopies (UV-*vis*, IR, and Raman). We expect that nanopore measurements will complement the characterization of these and other physical properties of POMs, as well as the study of their speciation at low concentration, which will help better understand the synthetic pathway of polyoxometalates formation. It was shown previously that the αHL pore can even distinguish between 2 isomers of the trivacant Keggin form $Na_8HPW_9O_{34}$.[30]

In conclusion, we have shown that a membrane-bound protein nanopore can be used to detect and characterize tungsten oxide metallic clusters (heteropolytungstates) in solution using a simple high resolution electrical measurement. The sensitivity afforded by this novel approach permits the tracking of subtle differences in POM structure that arise at different pH values at concentrations that are substantially lower (> 70-fold) than required for traditional methods such as NMR spectroscopy. Due to the single molecule detection capability of nanopores, the actual limit of detection in the method can be made much lower by measuring the current for longer times (the capture rate scales in proportion to the POM concentration).

DISCLOSURES:
None.

REFERENCES

1.   Bezrukov, S. & Kasianowicz, J. Current noise reveals protonation kinetics and number of

ionizable sites in an open protein ion channel. *Physical Review Letters* **70** (15), 2352–2355, doi:10.1103/PhysRevLett.70.2352 (1993).

2.   Kasianowicz, J. J. & Bezrukov, S. M. Protonation dynamics of the alpha-toxin ion channel from spectral analysis of pH-dependent current fluctuations. *Biophysj* **69** (1), 94–105, doi:10.1016/S0006-3495(95)79879-4 (1995).

3.   Please, T. R. & Ayub, M. *Solid-State Nanopore*. *Engineered Nanopores for Bioanalytical Applications*, 121–140, doi:10.1016/B978-1-4377-3473-7.00005-4 (Elsevier Inc.: 2013).

4.   Dekker, C. Solid-state nanopores. *Nature Nanotechnology* **2** (4), 209–215, doi:10.1038/nnano.2007.27 (2007).

5.   Kasianowicz, J. J., Brandin, E., Branton, D. & Deamer, D. W. Characterization of individual polynucleotide molecules using a membrane channel. *PNAS* **93** (24), 13770–13773, doi:10.1073/pnas.93.24.13770 (1996).

6.   Akeson, M., Branton, D., Kasianowicz, J. J., Brandin, E. & Deamer, D. W. Microsecond time-scale discrimination among polycytidylic acid, polyadenylic acid, and polyuridylic acid as homopolymers or as segments within single RNA molecules. *Biophysical Journal* **77** (6), 3227–3233, doi:10.1016/S0006-3495(99)77153-5 (1999).

7.   Singer, A. & Meller, A. Nanopore-based Sensing of Individual Nucleic Acid Complexes. *Israel Journal of Chemistry* **49** (3-4), 323–331, doi:10.1560/IJC.49.3-4.323 (2010).

8.   Jin, Q., Fleming, A. M., Burrows, C. J. & White, H. S. Unzipping kinetics of duplex DNA containing oxidized lesions in an α-hemolysin nanopore. *Journal of the American Chemical Society* **134** (26), 11006–11011, doi:10.1021/ja304169n (2012).

9.   Halverson, K. M., Panchal, R. G., *et al.* Anthrax biosensor, protective antigen ion channel asymmetric blockade. *Journal of Biological Chemistry* **280** (40), 34056–34062, doi:10.1074/jbc.M507928200 (2005).

10.   Oukhaled, G., Mathé, J., *et al.* Unfolding of proteins and long transient conformations detected by single nanopore recording. *Physical Review Letters* **98** (15), 158101, doi:10.1103/PhysRevLett.98.158101 (2007).

11.   Reiner, J. E., Kasianowicz, J. J., Nablo, B. J. & Robertson, J. W. F. Theory for polymer analysis using nanopore-based single-molecule mass spectrometry. *Proceedings of the National Academy of Sciences* **107** (27), 12080–12085, doi:10.1073/pnas.1002194107 (2010).

12.   Robertson, J. W. F., Rodrigues, C. G., Stanford, V. M., Rubinson, K. A., Krasilnikov, O. V. & Kasianowicz, J. J. Single-molecule mass spectrometry in solution using a solitary nanopore. *PNAS* **104** (20), 8207–8211, doi:10.1073/pnas.0611085104 (2007).

13.   Baaken, G., Ankri, N., Schuler, A.-K., Rühe, J. & Behrends, J. C. Nanopore-based single-molecule mass spectrometry on a lipid membrane microarray. *ACS Nano* **5** (10), 8080–8088, doi:10.1021/nn202670z (2011).

14.   Angevine, C. E., Chavis, A. E., Kothalawala, N., Dass, A. & Reiner, J. E. Enhanced single molecule mass spectrometry via charged metallic clusters. *Analytical Chemistry* **86** (22), 11077–11085, doi:10.1021/ac503425g (2014).

15.   Astier, Y., Uzun, O. & Stellacci, F. Electrophysiological study of single gold nanoparticle/alpha-Hemolysin complex formation: a nanotool to slow down ssDNA through the alpha-Hemolysin nanopore. *Small* **5** (11), 1273–1278,

doi:10.1002/smll.200801779 (2009).

16. Chavis, A. E., Brady, K. T., Kothalawala, N. & Reiner, J. E. Voltage and blockade state optimization of cluster-enhanced nanopore spectrometry. *Analyst* **140** (22), 7718–7725, doi:10.1039/C5AN01368B (2015).

17. Campos, E., McVey, C. E., Carney, R. P., Stellacci, F., Astier, Y. & Yates, J. Sensing single mixed-monolayer protected gold nanoparticles by the α-hemolysin nanopore. *Analytical Chemistry* **85** (21), 10149–10158, doi:10.1021/ac4014836 (2013).

18. Campos, E., Asandei, A., *et al.* The role of Lys147 in the interaction between MPSA-gold nanoparticles and the α-hemolysin nanopore. *Langmuir* **28** (44), 15643–15650, doi:10.1021/la302613g (2012).

19. Baaken, G., Halimeh, I., Bacri, L., Pelta, J., Oukhaled, A. & Behrends, J. C. High-Resolution Size-Discrimination of Single Nonionic Synthetic Polymers with a Highly Charged Biological Nanopore. *ACS Nano* **9** (6), 6443–6449, doi:10.1021/acsnano.5b02096 (2015).

20. Berzelius, J. J. Beitrag zur näheren Kenntniss des Molybdäns. *Annalen Der Physik* **82** (1), 369–392, doi:10.1002/andp.18260841202 (1826).

21. Long, D.-L., Burkholder, E. & Cronin, L. Polyoxometalate clusters, nanostructures and materials: from self assembly to designer materials and devices. *Chemical Society Reviews* **36** (1), 105–121, doi:10.1039/b502666k (2007).

22. Muller, A., Sessoli, R., *et al.* Polyoxovanadates: High-nuclearity spin clusters with interesting host-guest systems and different electron populations. Synthesis, spin organization, magnetochemistry, and spectroscopic studies. *Inorganic Chemistry* **36** (23), 5239–5250, doi:10.1021/ic9703641 (1997).

23. Rausch, B., Symes, M. D., Chisholm, G. & Cronin, L. Decoupled catalytic hydrogen evolution from a molecular metal oxide redox mediator in water splitting. *Science* **345** (6202), 1326–1330, doi:10.1126/science.1257443 (2014).

24. Dolbecq, A., Dumas, E., Mayer, C. R. & Mialane, P. Hybrid organic-inorganic polyoxometalate compounds: from structural diversity to applications. *Chemical Reviews* **110** (10), 6009–6048, doi:10.1021/cr1000578 (2010).

25. Busche, C., Vilà-Nadal, L., *et al.* Design and fabrication of memory devices based on nanoscale polyoxometalate clusters. *Nature* **515** (7528), 545–549, doi:10.1038/nature13951 (2014).

26. Pope, M. & Müller, A. *Polyoxometalates: From Platonic Solids to Anti-Retroviral Activity*. **10**, doi:10.1007/978-94-011-0920-8 (Springer Science & Business Media: Dordrecht, 2012).

27. Rhule, J. T., Hill, C. L., Judd, D. A. & Schinazi, R. F. Polyoxometalates in medicine. *Chemical Reviews* **98** (1), 327–358, doi:10.1021/cr960396q (1998).

28. Gao, N., Sun, H., *et al.* Transition-metal-substituted polyoxometalate derivatives as functional anti-amyloid agents for Alzheimer's disease. *Nature Communications* **5**, 3422, doi:10.1038/ncomms4422 (2014).

29. Pope, M. T. *Heteropoly and Isopoly Oxometalates*. **8** (Springer-Verlag Berlin Heidelberg: 1983).

30. Ettedgui, J., Kasianowicz, J. J. & Balijepalli, A. Single molecule discrimination of heteropolytungstates and their Isomers in solution with a nanometer-scale pore. *Journal*

       of the American Chemical Society **138** (23), 7228–7231, doi:10.1021/jacs.6b02917 (2016).

31.   Braha, O., Walker, B., *et al.* Designed protein pores as components for biosensors. *Chemistry & Biology* **4** (7), 497–505 (1997).

32.   Forstater, J. H., Briggs, K., *et al.* MOSAIC: A modular single-molecule analysis interface for decoding multistate nanopore data. *Analytical Chemistry* **88** (23), 11900–11907, doi:10.1021/acs.analchem.6b03725 (2016).

33.   Misakian, M. M. & Kasianowicz, J. J. J. Electrostatic influence on ion transport through the alphaHL channel. *Journal of Membrane Biology* **195** (3), 137–146, doi:10.1007/s00232-003-0615-1 (2003).